GT2015-43127

STABILITY CRITERIA FOR STANDING AND SPINNING WAVES IN ANNULAR COMBUSTORS

Giulio Ghirardo[*]
Matthew P. Juniper
University of Cambridge
Engineering department
Trumpington street CB2 1PZ Cambridge, UK
Email: giulio.ghirardo@gmail.com

Jonas P. Moeck
Institut für Strömungsmechanik und Technische Akustik
Technische Universität Berlin
Müller-Breslau-Strasse 8,10623 Berlin, Germany

ABSTRACT

Rotationally symmetric annular combustors are of practical importance because they generically resemble combustion chambers in gas turbines and aeroengines, in which thermoacoustically driven oscillations are a major concern. We focus on thermoacoustic oscillations of azimuthal type, neglect the effect of the transverse acoustic velocity in the azimuthal direction, and model the heat release rate as being dependent only on the pressure in the combustion chamber. We study the dynamics of the annular combustor with a finite number of compact flames equispaced along the annulus, and characterise the flames' response with a describing function. We discuss with broad generality the existence, amplitudes and the stability of standing and spinning waves, as a function of: 1) the number of the burners; 2) the damping in the chamber; 3) the flame describing function. These have implications on industrial applications, the future direction of investigations, and for what to look for in experimental data. We then present as an example of application the first theoretical study of triggering in annular combustors, and show that rotationally symmetric annular chambers can experience stable standing solutions.

NOMENCLATURE

A_1, A_2 slowly varying amplitudes of the 2 standing modes
A^{sp} amplitude of a spinning wave that is solution of the problem

A^{st} amplitude of a standing wave that is solution of the problem
G gain of the flame response
N_b Number of identical burners in the annular chamber
$\mathbb{Q}$ time-domain operator characterising the response of q to the pressure p
Q describing function of the response of q to the pressure p
$\text{Re}[Q]$ part of the flame response in phase with the pressure p
R_j slowly varying amplitude of the pressure field along the annulus at the j-th burner
R_j^{st} slowly varying amplitude of the pressure field along the annulus at the j-th burner for a standing mode
R_j^{sp} slowly varying amplitude of the pressure field along the annulus at the j-th burner for a spinning mode
R_{max} maximum amplitude of oscillation of a spinning or standing solution, in the span of a limit-cycle and along the annulus.
c_j, s_j cosine and sine functions, calculated at the azimuthal position θ_j of the j-th burner
p non-dimensionalised pressure field
q non-dimensionalised heat release rate
r radial distance in cylindrical coordinates
$\bar{r}$ radial distance of the burners from the z axis
$\boldsymbol{x}$ point in the 3D domain in cylindrical coordinates, $\boldsymbol{x} = (z, r, \theta)$
z height in cylindrical coordinates
α equivalent acoustic damping of the annular chamber
$\Delta\theta$ angle between a burner and the next in the azimuthal direction, i.e. $\Delta\theta = 2\pi/N_b$

---

[*]Address all correspondence to this author

ζ parameter fixing the position of the pressure anti-node of a standing wave

$\eta_1(t), \eta_2(t)$ instantaneous amplitudes of the 2 standing modes

θ azimuthal coordinate in cylindrical coordinate, $\theta \in [0, 2\pi]$

θ_j value of the azimuthal coordinate of the j-th burner

ϕ phase of the flame response

φ_1, φ_2 slowly varying phases of the 2 standing modes

φ phase difference $\varphi_1 - \varphi_2$ between the 2 standing modes

$\psi_1(\boldsymbol{x}), \psi_2(\boldsymbol{x})$ complex-valued eigenmode of the lin. problem

ω non-dimensionalised natural frequency of oscillation of the 2 oscillators

Ω spatial domain of the combustion chamber

INTRODUCTION

This paper tackles the problem of thermoacoustic instabilities in annular combustors, and particularly the nonlinear saturation of these instabilities to a limit-cycle. Large eddy simulations [1,2,3] and laboratory scale experiments [4,5,6,7,8] present both spinning waves, rotating either clockwise or anticlockwise in the annulus, and standing waves, with pressure and velocity nodes fixed in space. At the moment it is unclear what are the governing factors leading to standing vs spinning solutions.

We focus on rotationally symmetric annular chambers, because the effect of a deviation from rotational symmetry has already been studied and can lead to stable standing solutions [9].

All[1] low-order studies on rotationally symmetric annular chambers have modelled the flame response as a function of the local value of the acoustic pressure in the annular chamber, or as a function of the longitudinal acoustic velocity in the burner. They have shown that spinning waves were the only stable solution of the problem for specific families of heat release rate responses, viz. monotonously saturating static nonlinearities [11,12,13].

This article shows how to exploit the knowledge of the describing function of one burner to work out whether or not spinning and standing modes are stable, by applying a weakly nonlinear analysis and the method of averaging.

We carry out the analysis for a generic describing function, and obtain results that are mostly in line with the existing literature, though we show how and why standing solutions can be stabilized[2], and provide illustrative explanations for the complex dynamics. We also provide measurable quantities in experimental data to study standing modes, which allow to test the validity of the hypotheses of this model.

---

[1] with one exception, [10], discussed later

[2] here and in the following standing and spinning solutions are limit-cycles of the problem, so that for example a stabilized standing solution is a stable limit-cycle, not a standing eigenmode of the problem with negative growth-rate.

PROBLEM GEOMETRY

We study an annular combustion chamber and adopt cylindrical coordinates z, r, θ, with the axis z corresponding to the axis of symmetry of the chamber, and θ in $[0, 2\pi]$. We assume that a number N_b of equal burners are equispaced along the annulus by an angle $\Delta\theta \equiv 2\pi/N_b$. We neglect the effect of a mean azimuthal velocity U_θ. Refer to [14] for a detailed analysis of this effect in a linear framework, still under the assumption that U_θ does not affect the flames. We assume the flames to be compact so that the fluctuating heat release rate is concentrated at the locations of the burners:

$$q(\boldsymbol{x},t) = \sum_{j=0}^{N_b-1} q_j(t)\delta(\boldsymbol{x} - \boldsymbol{x}_j) \quad \boldsymbol{x} \equiv (z,r,\theta) \; , \; \boldsymbol{x}_j \equiv (0,\overline{r},\theta_j) \quad (1)$$

where δ is the Dirac delta, $\overline{r}$ is the radial position of the burners, and the plane $z = 0$ is at the interface between the combustion chamber and the burners, which are located at the azimuthal positions θ_j, given by:

$$\theta_j \equiv \mathrm{mod}\left[\overline{\theta} + j\Delta\theta, 2\pi\right] \quad , \quad N_b \geq 4, \; j = 0, 1, \ldots, N_b - 1 \quad (2a)$$

$$\overline{\theta} \equiv \frac{\pi}{4} + \frac{\Delta\theta}{4}\zeta \quad \begin{cases} \zeta \in \{0,2\} & \text{if } N_b \text{ is even} \\ \zeta \in \{0,1,2,3\} & \text{if } N_b \text{ is odd} \end{cases} \quad (2b)$$

where $\mathrm{mod}[x, 2\pi]$ is the remainder of the division of x by 2π. We assume $N_b \geq 4$, which is satisfied for practically relevant configurations. The addition of the constant $\overline{\theta}$ and of the coefficient ζ is arbitrary, and corresponds to a simple rotation of the frame of reference, which will be useful later. For the time being, it suffices to observe from (2) that the position at the angle $\theta = \pi/4$:

for $\zeta = 0$ is occupied by a burner;
for $\zeta = 2$ is equispaced between 2 adjacent burners;
for $\zeta = 1$ is $3\Delta\theta/4$ far from the preceding burner and $\Delta\theta/4$ far from the next.

FLAME RESPONSE

We assume that the heat release rate q_j of the j-th flame depends on the local perturbation field only. A successful and common modelling approach consists of expressing q_j in terms of only the acoustic axial velocity v_j in the burner upstream of the flame. Doing so, we assume that the mean azimuthal velocity U_θ has a negligible effect on the axisymmetry of the mean flame shape, and more in general that the azimuthal, acoustic velocity u does not affect the response. This last point is proved theoretically in the linear limit for axisymmetric premixed flames in [15], and the effect of the loss of axisymmetry is discussed in [16]. The effect is experimentally verified to be small at low amplitudes of transverse forcing, for the cases of a burner positioned at pressure/velocity nodes, and for the case where it is

swept by a spinning wave, where both u and v are excited at the same time [17] (refer also to [18] for a linear discussion of the transverse, forced flame response in frequency domain and a literature review). This effect is usually not taken into account because little is known in the nonlinear regime, i.e. at large amplitudes of oscillation typical of self-excited thermoacoustic oscillations. In this paper we make the same assumption, but point out that the nonlinear effect of the transverse azimuthal velocity u on each flame has been investigated in [10]. It does not affect the linear stability properties of the system, but it does however affect the nonlinear dynamics, and can stabilize[2] standing modes in axisymmetric annular chambers.

The longitudinal fluctuating velocity v_j oscillating in the j-th burner is related to the acoustic pressure difference Δp_j between the two sides of the burner, which are the chamber and the plenum, under the assumption of burner's acoustic compactness [19], that allows the modelling of the burner as a lumped element. However, if we consider 1 mode oscillating harmonically in time, and we assume that the burner transfer function of the lumped element is linear with the amplitude of oscillation (as validated for example in [20]), we have that Δp_j is proportional to p_j, and one can express v_j as a function of the local value of the pressure in the chamber p_j. The same reasoning applies if a pair of degenerate azimuthal modes oscillate at the same frequency, as will be the case in the following. We then model the heat release rate q_j as a function depending on p_j instead of v_j. In particular, we model the heat release response as a nonlinear, time-invariant operator $\mathcal{Q}$:

$$q_j(t) = \mathcal{Q}[p_j(t)] \tag{3}$$

The time-domain operator $\mathcal{Q}$ contains all the complexity of the relation between p_j and q_j. We restrict our study to operators $\mathcal{Q}$ that, excited with a harmonic input $p = A\cos(\omega t)$, respond strongly at the same input frequency ω and weakly at higher harmonics $2\omega, 3\omega, \ldots$. This assumption is usually called the filtering hypothesis [21]. We observe however that this is a feature of flames, acting like a low-pass filter on the acoustic input [22], and is one of the reasons why frequency domain formulations have proven successful in thermoacoustics even for limit-cycles calculations.

We will study the problem both in the time domain and in the frequency domain. We refer with the calligraphic symbol $\mathcal{Q}$ to the the time domain operator. This operator in the frequency domain is characterized here by the sinusoidal-input describing function, which we denote with the upper-case Q, defined as:

$$Q(A,\omega) \equiv \frac{1}{A}\frac{1}{\pi/\omega}\int_0^{2\pi/\omega}\mathcal{Q}\left[A\cos(\omega t)\right]e^{i\omega t}dt \tag{4}$$

The real part and the imaginary part of $Q(A,\omega)$ express the am-

plitudes of the components of the output of $\mathcal{Q}$ respectively in phase and in quadrature with the sinusoidal pressure input. In particular it is the real part of Q that leads to a contribution to the energy production term $q(t)p(t)$ in the Rayleigh criterion: if positive, the contribution is positive. One can then define the gain G and the phase φ of the flame response as the polar coordinates of the complex number $Q(A,\omega)$:

$$Q(A,\omega) = G(A,\omega)e^{i\phi(A,\omega)} \tag{5}$$

$$\begin{cases} G(A,\omega) & = |Q(A,\omega)| \\ \phi(A,\omega) & = \arg[Q(A,\omega)] \end{cases} \tag{6}$$

GOVERNING EQUATIONS

The governing equations of the problem were already derived in [11, 9, 10] for a specific heat release response uniformly distributed in the azimuthal direction. In this article the heat release response is concentrated at discrete positions and we keep the flame response generic. The resulting equations are only slightly different, and are reported in (12) and (13). The starting point in these references are the fluctuating momentum and fluctuating energy equation, in the time-domain, and a reasonable, phenomenological choice of a truncated Galerkin basis.

On the contrary here we study the problem as weakly nonlinear, by assuming that the solution of the nonlinear problem is a perturbation of the solution of the linearized problem, in frequency domain:

$$\hat{p}(\boldsymbol{x},\omega) = [\hat{\eta}_1(\omega)\psi_1(\boldsymbol{x}) + \hat{\eta}_2(\omega)\psi_2(\boldsymbol{x}) + c.c.] + \varepsilon\hat{p}_\varepsilon(\boldsymbol{x},\omega) \tag{7}$$

The two complex-valued modes $\psi_1(\boldsymbol{x})$ and $\psi_2(\boldsymbol{x})$ are standing eigenmodes of the linearised, neutrally stable problem, and at the burners positions they are proportional respectively to $\cos\theta$ and $\sin\theta$. We normalise the 2 modes so that at the burners' position, along the annulus the pressure field in time-domain is

$$p\big(\boldsymbol{x} = (0,\bar{r},\theta_j),t\big) = [\eta_1(t)\cos\theta_j + \eta_2(t)\sin\theta_j] + \varepsilon\hat{p}_\varepsilon(\boldsymbol{x},t) \tag{8}$$

The $\eta_1(t)$ and $\eta_2(t)$ coefficients are the instantaneous amplitudes of the 2 standing modes, and ε expresses the deviation of the weakly nonlinear nonlinear solution from the exact solution. By neglecting the correction $\varepsilon\hat{p}_\varepsilon(\boldsymbol{x})$ we recover the coupled oscillators already derived in [9].

The details of the weakly nonlinear analysis are lengthy, and not reported due to the page limit of this publication. The following serves as a trace, sufficient to reproduce the results to people familiar with this type of analysis. We substitute (7) in the damped Helmholtz equation with heat source. We multiply by the complex conjugate ψ_1^* and integrate over the domain. In

general, the eigenmodes are not orthogonal [23]. However, azimuthal modes in rotationally symmetric combustion chambers are degenerate with geometric multiplicity 2, and share the same frequency. Exploiting the orthogonality of the 2 modes and then taking the inverse Fourier transform we obtain (9a):

$$\frac{\partial^2 \eta_1(t)}{\partial t^2} + \alpha \frac{\partial \eta_1(t)}{\partial t} + \omega^2 \eta_1(t) = \tag{9a}$$

$$\sum_{j=0}^{N_b-1} \frac{\partial}{\partial t} \mathcal{Q} [\eta_1(t)c_j + \eta_2(t)s_j] \mu c_j + O(\varepsilon)$$

$$\frac{\partial^2 \eta_2(t)}{\partial t^2} + \alpha \frac{\partial \eta_2(t)}{\partial t} + \omega^2 \eta_2(t) = \tag{9b}$$

$$\sum_{j=0}^{N_b-1} \frac{\partial}{\partial t} \mathcal{Q} [\eta_1(t)c_j + \eta_2(t)s_j] \mu s_j + O(\varepsilon)$$

where equation (9b) has been obtained similarly but by multiplying by ψ_2^* instead of ψ_1^*, and we introduced the notation

$$\begin{cases} c_j & \equiv \cos \theta_j \\ s_j & \equiv \sin \theta_j \end{cases} \tag{10}$$

The coefficients α and ω are respectively an equivalent damping coefficient and the natural frequency of the oscillators, and are both calculated in the linearised problem, and the coefficient μ is a normalisation constant:

$$\mu = \left[\int_\Omega \psi_1(\boldsymbol{x}) \psi_1(\boldsymbol{x})^* d\Omega \right]^{-1} \tag{11}$$

where Ω is the combustion chamber's domain. In the following we set $\mu = 1$, because it can be incorporated in the operator $\mathcal{Q}$.

For simplicity of notation, we indicate the derivative with respect to the time variable t simply with a prime. We neglect terms of order $O(\varepsilon)$ and recast the system (9) in the form:

$$\eta_1'' + \alpha \eta_1' + \omega^2 \eta_1 = f_1(\eta_1, \eta_2) \tag{12a}$$

$$\eta_2'' + \alpha \eta_2' + \omega^2 \eta_2 = f_2(\eta_1, \eta_2) \tag{12b}$$

where the functions f_i at the RHS are:

$$f_1(\eta_1, \eta_2) = \sum_{j=0}^{N_b-1} \mathcal{Q}' [\eta_1 c_j + \eta_2 s_j] c_j \tag{13a}$$

$$f_2(\eta_1, \eta_2) = \sum_{j=0}^{N_b-1} \mathcal{Q}' [\eta_1 c_j + \eta_2 s_j] s_j \tag{13b}$$

We then assume the terms $f_i(\eta_1, \eta_2) - \alpha \eta_i'$ to be small in both oscillators and apply the method of averaging to the state-space model (12). The resulting dynamic equations, which evolve on a slower timescale, are called the slow flow equations of the problem. They describe the temporal evolution of the solution in terms of the slowly varying amplitudes A_1 and A_2 of the 2 standing modes and of their phase difference $\varphi \equiv \varphi_1 - \varphi_2$, by which we can rewrite the expression of the pressure field described in (8):

$$p(\theta, t) = A_1 \cos(\omega t + \varphi_1) \cos \theta + A_2 \cos(\omega t + \varphi_2) \sin \theta \tag{14}$$

where the A_i and φ_i are slowly varying time variables, of a slower timescale T. The slow flow equations are:

$$A_1' = -\frac{\alpha}{2} A_1 + \frac{1}{2} \sum_{j=0}^{N_b-1} G(R_j, \omega) \left[A_1 c_j^2 \cos \phi(R_j, \omega) + A_2 c_j s_j \cos(\phi(R_j, \omega) + \varphi) \right] \tag{15a}$$

$$A_2' = -\frac{\alpha}{2} A_2 + \frac{1}{2} \sum_{j=0}^{N_b-1} G(R_j, \omega) \left[A_2 s_j^2 \cos \phi(R_j, \omega) + A_1 c_j s_j \cos(\phi(R_j, \omega) - \varphi) \right] \tag{15b}$$

$$\varphi' = \frac{1}{2} \sum_{j=0}^{N_b-1} G(R_j, \omega) \left[(s_j^2 - c_j^2) \sin \phi(R_j, \omega) - c_j s_j \left(\frac{A_2}{A_1} \sin(\phi(R_j, \omega) + \varphi) - \frac{A_1}{A_2} \sin(\phi(R_j, \omega) - \varphi) \right) \right] \tag{15c}$$

We study these equations to calculate the amplitudes of the solutions, their spatial structure and their stability. The quantity R_j in (15) is the local amplitude of oscillation of pressure at the j-th burner:

$$R_j(A_1, A_2, \varphi) = \sqrt{(A_1 c_j)^2 + (A_2 s_j)^2 + 2A_1 A_2 c_j s_j \cos(\varphi)} \quad (16)$$

where the terms $A_1 c_j$ and $A_2 s_j$ are the amplitudes of the pressure of the 2 modes η_1, η_2 at the position θ_j. The quantity R_j is the argument of the flame gain G and of the flame phase response ϕ, which both in turn govern the nonlinear saturation effect. This means that small values of R_j lead to a quasi-linear response of the j-th burner, while large values of R_j lead to a strongly nonlinear response.

We restrict the domain of study of the problem to $(A_1, A_2, \varphi) \in \mathbb{R}^+ \times \mathbb{R}^+ \times [0, \pi)$ by exploiting the symmetries of the equations.

In the following section we discuss the structure of standing and spinning waves. Notice that *waves* are here considered as possible initial conditions of the problem at hand at a certain instant of time, and the system can drift away from this initial state as time evolves. We oppose these to standing and spinning *solutions*, which are waves that are also periodic solutions of the problem. The amplitude of oscillation of these solutions is considered in the following section. A third section discusses finally the stability of these solutions. A section with an example application follows.

STANDING AND SPINNING WAVES

We prove in this section that a point with coordinates $(A_1, A_2, \varphi) = (A, A, k\pi/2)$ is always a standing or a spinning wave:

$$(A, A, k\pi/2) \begin{cases} k \text{ even} \Leftrightarrow p(\theta, t) \text{ is a standing wave} \\ k \text{ odd} \Leftrightarrow p(\theta, t) \text{ is a spinning wave} \end{cases} \quad (17)$$

Spinning wave

A spinning wave of amplitude A travels with a phase speed equal to ∓ 1 either in clockwise/anticlockwise direction:

$$\begin{aligned} p &= A\cos(\omega t + \varphi_1 \pm \theta) \\ &= A\cos(\omega t + \varphi_1)\cos\theta + A\cos(\omega t + \varphi_1 \pm \pi/2)\sin\theta \end{aligned} \quad (18)$$

By comparing this with (14), we observe that for a spinning wave we have $A = A_1 = A_2$ and $\varphi = \pm \pi/2$, with the $\pm$ sign respectively for a mode rotating in the counter-clockwise or clockwise direction. We present in Figure 1 the pressure field $p(\theta, t)$ obtained from (18), nondimensionalized with respect to the amplitude A, at 2 instants of time. As the wave moves to the right

(anticlockwise direction), it maintains the same amplitude of oscillation. We now simplify the expression $R_j(A_1, A_2, \varphi)$ by sub-
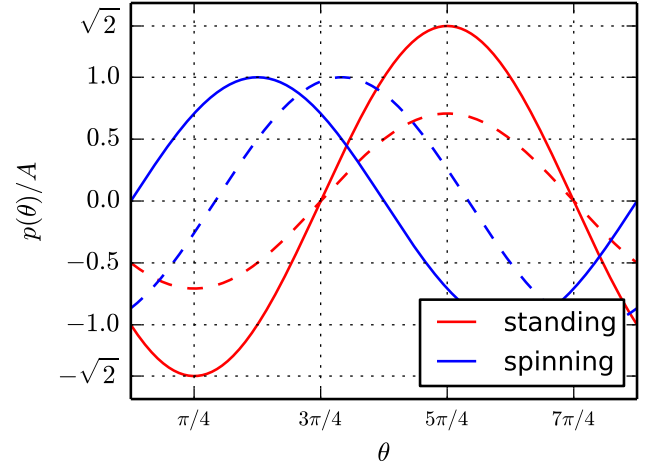

FIGURE 1: PRESSURE FIELD OF A SPINNING WAVE (BLUE) FROM EQUATION (18) AND OF A STANDING WAVE (RED) FROM EQUATION (20) AT 2 INSTANTS OF TIME.

stituting $A_1 = A_2$ and $\varphi = \pi/2$ in (16), obtaining

$$R_j^{sp} = A \quad (19)$$

This means that the amplitude of oscillation of a spinning wave is constant along the annulus, see Figure 2.

Standing wave

A standing wave has velocity and pressure nodes fixed in time, i.e.

$$p = \sqrt{2}A\cos(\omega t + \varphi_1)\cos(\theta - \pi/4) \quad (20)$$

where the $\sqrt{2}$ factor will be explained later, and we decided to choose a frame of reference with a pressure anti-node at $\bar{\theta} = \pi/4$. This can be rewritten as

$$p = A\cos(\omega t + \varphi_1)\cos\theta + A\cos(\omega t + \varphi_1)\sin\theta \quad (21)$$

By comparing (21) with (14), we observe that we have $(A_1, A_2, \varphi) = (A, A, 0)$. This is why we put a $\sqrt{2}$ factor in equation (20) in the first place. We present in Figure 1 the pressure
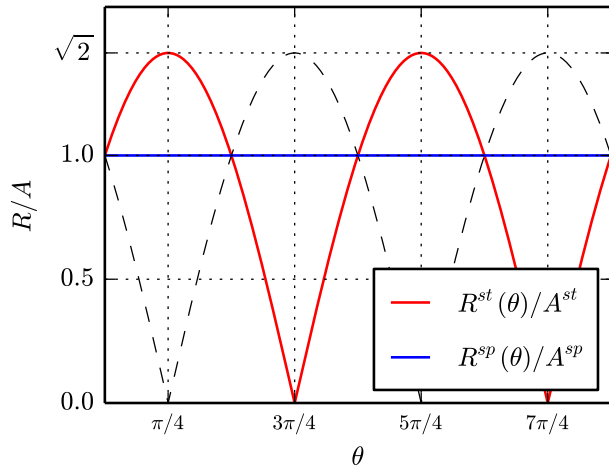
FIGURE 2: AMPLITUDE OF OSCILLATION OF A STANDING WAVE (RED LINE) FROM EQUATION (22) AND OF A SPINNING WAVE (BLUE LINE) FROM EQUATION (19). THE DASHED LINE IS THE AMPLITUDE OF THE VELOCITY FIELD OF A STANDING WAVE. THESE AMPLITUDES ARE CONSTANT IN TIME, AS OPPOSED TO THE PRESSURE FIELDS IN FIGURE 1.

field $p(\theta, t)$ obtained from (20), non-dimensionalized with respect to the amplitude A, at 2 instants of time $t = -\varphi_1/\omega$ (continuous red line) and $t + \Delta t = -(\varphi_1 + \pi/3)/\omega$ (dashed red line). The position of the pressure nodes is fixed in space.

   We can prove that if the number of burners N_b is *even* there can be a total of N_b distinct standing waves that are solutions. Half of these standing solutions present one of their pressure anti-nodes at the position of one burner, and the others present one of their pressure anti-nodes exactly between 2 burners. Their velocity nodal lines are reported respectively in black and grey in Figure 3.a. This is consistent with the standing modes observed in the MICCA annular combustor at the laboratoire EM2C (Ecole Centrale Paris), equipped with 16 burners. When the burners are of the swirl type, the standing modes are highly stochastic, but the nodal line exhibits a preferential position between 2 burners [7]. When equipped with matrix burners, the system is less stochastic and the velocity nodal line stays again between 2 burners [24, 25].

   We can prove that if the number of burners N_b is *odd* there can be a total of $2N_b$ distinct standing waves that are solutions. Half of these standing solutions present one pressure anti-node exactly between 2 burners and the other pressure anti-node at one burner on the opposite side. Their velocity nodal lines are reported in black in Figure 3.b. The other standing solutions present both pressure anti-nodes distant $\Delta\theta/4$ from 2 different

burners, and their velocity nodal lines are reported in gray in the figure.

(a) EVEN NUMBER OF BURNERS, E.G. HERE $N_b = 16$
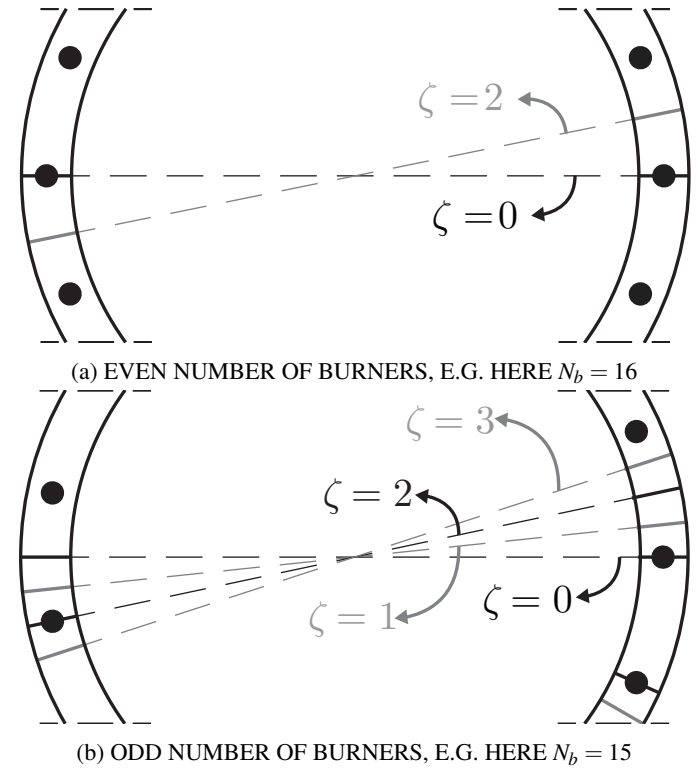

(b) ODD NUMBER OF BURNERS, E.G. HERE $N_b = 15$

FIGURE 3: POSITION OF THE VELOCITY NODAL LINES OF ALL POSSIBLE STANDING SOLUTIONS. THE VELOCITY NODAL LINES LINK 2 PRESSURE ANTI-NODES, AND ONLY THE LINES FULLY CONTAINED IN THIS SECTION ARE REPORTED. THE BURNERS ARE REPRESENTED WITH LARGE BLACK DISCS, AND THE SEMI-CIRCLES ARE THE INTERNAL AND EXTERNAL WALLS OF THE CHAMBER. IN a) THE NUMBER OF BURNERS N_b IS EVEN AND EACH BURNER FACES ANOTHER BURNER ON THE OTHER SIDE OF THE ANNULUS. IN THE ANGLE $\Delta\theta = 2\pi/N_b$ WE HAVE ONE BLACK AND ONE GRAY LINE FOR A TOTAL OF 2 STANDING WAVES FOR EACH BURNER. IN B) THE NUMBER OF BURNERS IS ODD, AND EACH BURNER FACES THE SPACE BETWEEN 2 OTHER BURNERS ON THE OTHER SIDE OF THE ANNULUS. THERE ARE A TOTAL OF 4 STANDING WAVES FOR EACH BURNER.

   We decide, instead of studying in a fixed frame of reference all the possible standing waves with different orientations just presented, to study each standing wave in an ad-hoc rotated frame of reference where $A_1 = A_2$. This means that at $\theta = \pi/4$

the mode presents a pressure anti-node. By varying the value of ζ in (2), we can choose to study a mode with a pressure anti-node at different positions, as discussed just below equation (2) and sketched in Figure 3.

We then evaluate the structure of $R_j(A_1, A_2, \varphi)$ by substituting in (16) the expressions (17). We obtain

$$R_j^{st} = A\sqrt{1 + \sin(2\theta_j)} = \sqrt{2}A|\cos(\theta_j - \pi/4)| \qquad (22)$$

The amplitude of oscillation R is maximum at $\theta_j = \pi/4$, where pressure anti-nodes are located, and zero at pressure nodes. This can be observed in Figure 2, where we present the pressure amplitude of oscillation R with a continuous red line as a continuous function of θ.

In the following, we will discuss the amplitudes of the 2 modes in terms of their maximum amplitude in space and time. They are trivially

$$R_{max}^{sp} = A^{sp} \qquad (23a)$$
$$R_{max}^{st} = A^{st}\sqrt{2} \qquad (23b)$$

AMPLITUDES OF SPINNING AND STANDING SOLUTIONS

The standing and spinning waves introduced in the previous section are solutions of the problem only if $(A_1, A_2, k\pi/2) = (A, A, k\pi/2)$ is a fixed point[3] of (15). This means that standing and spinning waves $(A, A, k\pi/2)$, though valid initial condition of the problem, are not necessarily solutions, and the system may drift away from such an initial condition.

Spinning solution

We prove that there exists a spinning wave with amplitude A that is solution of the problem if we can solve the equation:

$$F^{sp}(A) = \alpha \qquad (24)$$

where we introduced

$$F^{sp}(A) \equiv \frac{N_b}{2} \mathrm{Re}\left[Q(A, \omega)\right] \qquad (25)$$

Notice how $\mathrm{Re}\left[Q(A), \omega\right]$ is the component of the response of the flame that is in phase with the pressure p on the limit-cycle. It

_____

[3]notice that the equations (15) are the averaged equations of (9), so that a fixed point of (15) is a limit-cycle of (9), and in turn it is an oscillatory pressure field (of the original partial differential equation) that is a solution.

is possible to prove that the condition (24) can be obtained from the Rayleigh criterion:

$$\int_\Omega \int_T \left[q(\boldsymbol{x},t) - \alpha p(\boldsymbol{x},t)\right] p(\boldsymbol{x},t) dt d\Omega = 0. \qquad (26)$$

Standing solution

We prove that there exists a standing wave with amplitude A if we can solve the equation:

$$F^{st}(A) = \alpha \qquad (27)$$

where we introduced

$$F^{st}(A) \equiv \frac{1}{2} \sum_{j=0}^{N_b-1} (1 + \sin(2\theta_j)) \mathrm{Re}\left[Q\left(A\sqrt{1 + \sin(2\theta_j)}\right)\right] \qquad (28)$$

Also in this case, the condition (27) can be obtained from the Rayleigh criterion (26).

STABILITY OF SPINNING AND STANDING SOLUTIONS

By calculating the eigenvalues of the Jacobian of the system (15), we can establish necessary and sufficient conditions for the stability[2] of the solutions. These calculations are too long even to be reported in an appendix, and do not add physical insight to the problem.

Stable spinning solutions

We find that a spinning solution with amplitude A^{sp} is stable if and only if

$$\mathrm{Re}\left[Q'(A^{sp})\right] < 0 \qquad (29)$$

In the equation, the prime indicates a derivative with respect to the argument A. Notice that this condition could be obtained by deriving with respect to the amplitude A the Rayleigh criterion (26). It follows that the condition (29) requires the flame response to be weaker than the damping at amplitudes larger than A^{sp}, and stronger than the damping at amplitudes smaller than A^{sp}. This condition is the same stability condition as that of stable thermoacoustic limit-cycles in longitudinal configurations, and has a very intuitive physical interpretation.

Moreover, notice that if one assumes that the flame does not extinguish, (i.e. formally that the describing function is defined and continuous at all amplitudes, and that the gain eventually goes to zero at infinite amplitudes) and that the damping is not

large enough to kill off completely thermoacoustic instabilities (granted in all cases of interest), then there necessarily exists a stable spinning solution, whatever the flame response is.

This has a few implications for a combustor exposed to a reasonably high degree of background noise with a reasonably large number of burners, which is the typical industrial case:

1. the dynamic state of a rotationally symmetric combustor will spend some intervals of time in the vicinity of the spinning solutions, and one pressure sensor will be sufficient to detect if the system is undergoing a thermoacoustic instability.
2. if a combustor, pushed by the background noise, does not

present a spinning solution as a noisy attractor, either it is not rotationally symmetric, or some other factor is playing a key role in the dynamics. One factor that has already been investigated is transverse forcing [10]. Other factors may contribute as well: little is know on dynamical effects of the temperature distribution.

Stable standing solutions

There are 3 necessary and sufficient conditions for the stability of a standing solution with amplitude A^{st}:

$$F^{st\prime}(A^{st}) < 0 \tag{30a}$$

$$\left[\sum_{j=0}^{N_b-1} c_j s_j \text{Re}\left[Q(A^{st}\sqrt{1+2c_js_j}, \omega)\right] - A^{st}\frac{1}{4}\sum_{j=0}^{N_b-1}\frac{(c_j^2-s_j^2)^2}{\sqrt{1+2c_js_j}}\text{Re}\left[Q'(A^{st}\sqrt{1+2c_js_j}, \omega)\right] \right]\left[\sum_{j=0}^{N_b-1} c_j s_j \text{Re}\left[Q(A^{st}\sqrt{1+2c_js_j}, \omega)\right] \right] +$$

$$\left[\sum_{j=0}^{N_b-1} c_j s_j \text{Im}\left[Q(A^{st}\sqrt{1+2c_js_j}, \omega)\right] - A^{st}\frac{1}{4}\sum_{j=0}^{N_b-1}\frac{(c_j^2-s_j^2)^2}{\sqrt{1+2c_js_j}}\text{Im}\left[Q'(A^{st}\sqrt{1+2c_js_j}, \omega)\right] \right]\left[\sum_{j=0}^{N_b-1} c_j s_j \text{Im}\left[Q(A^{st}\sqrt{1+2c_js_j}, \omega)\right] \right] > 0 \tag{30b}$$

$$\sum_{j=0}^{N_b-1} c_j s_j \text{Re}\left[Q(A^{st}\sqrt{1+2c_js_j}, \omega)\right] - A^{st}\frac{1}{8}\sum_{j=0}^{N_b-1}\frac{(c_j^2-s_j^2)^2}{\sqrt{1+2c_js_j}}\text{Re}\left[Q'(A^{st}\sqrt{1+2c_js_j}, \omega)\right] > 0 \tag{30c}$$

In the equations, the prime indicates a derivative with respect to the argument A. The first condition (30a) follows exactly the same interpretation of the condition (29) for the spinning solution: if a standing mode is stable, at amplitudes larger then A^{st} the damping losses are larger than the energy gains. Again, this can be explained with the derivative of the Rayleigh criterion with respect to the amplitude A^{st} of oscillation.

We now consider the asymptotic limit for a large number of burners of the second (30b) and third (30c) condition because it will provide both a simplification and the interpretation of the 2 conditions. In the limit $N_b \to \infty$, we have that the summations can be replaced by integrals in θ over the domain $[0, 2\pi]$, and we recover a uniformly distributed heat release rate model, more common in the literature [11, 9, 10]. For a large number of burners, flame merging may occur, and would change the describing function Q of the individual flames. The analysis still holds, but in the following results one should interpret Q as the describing function of the ensemble response of an infinitely small wedge of the annulus, populated by many flames.

One can prove that the second condition (30b) simplifies to $0 > 0$ for $N_b \to \infty$, and it is not respected, and the standing so-

lution is not stable. However, the standing solution is neutrally stable, because for neutral stability the condition (30b) evaluates to $0 \geq 0$. This means that the standing mode solution is insensitive to a shift of the fixed point in a certain direction, which is a rotation of the nodal line of an arbitrary angle in the azimuthal direction. This neutral stability of standing solutions is known in models with uniformly distributed heat release rate, as discussed in [10], and obviously can be traced back to the axisymmetry of the problem for $N_b \to \infty$. On the other hand, for a finite number of burners we have a fixed number of possible positions of the nodal lines (see Figure 3), and the condition (30b) discusses if a certain family of standing solutions is stable/unstable in the azimuthal direction.

The third condition, in the limit $N_b \to \infty$, and generalized to a thermoacoustic mode with azimuthal wavenumber[4] n, simplifies to

$$N_{2n} \equiv \int_0^{2\pi} \text{Re}\left[Q(A^{st}\sqrt{1+\sin(2n\theta)}, \omega)\right]\sin(2n\theta)d\theta \geq 0 \tag{31}$$

---

[4] i.e. the number of periods of the mode in the azimuthal direction θ between 0 and 2π.

8

We recall that $Q(A, \omega)$ is the describing function of the flame response to a harmonic input of amplitude A, and ω is the frequency of the standing solution. The argument $A^{st}\sqrt{1 + \sin(2\theta)}$ is the spatial distribution of the pressure amplitude of oscillation of the standing solution reported in red in Figure 2.

Before discussing further the condition (31), we recall from [9] the quantity[5]:

$$C_{2n} = \int_0^{2\pi} \text{Re}[Q_\theta(0, \omega)] \sin(2n\theta) d\theta \qquad (32)$$

This coefficient C_{2n} is the harmonic at 2θ of the linear heat release response[6] along the annulus, and n is the azimuthal wavenumber[4] of the oscillation. In the integral (32) the linear response Q_θ depends directly on the azimuthal angle θ, while in the integral (31) the response depends only indirectly on the azimuthal angle through the amplitude of the forcing $A^{st}\sqrt{1 + \sin(2\theta)}$. Noiray et al. [9] consider a simple heat release response $q = \beta(\theta)p - p^3$, and prove that:

1. for a rotationally symmetric chamber $C_{2n} = 0$ the system stabilizes towards a spinning solution,
2. for small asymmetry in the $2n\theta$ component, i.e. for intermediate values of C_{2n}, the system stabilizes to a mixed spinning/standing mode
3. for large asymmetry, in the $2n\theta$ component, i.e. large values of C_{2n}, the system stabilizes to a standing mode

The coefficient C_{2n} is a linear property of the system (in the sense that it describes the azimuthal variation of the transfer functions of the flames, that are linear operators): only the specific loss of rotational symmetry in the 2θ component affects the nature of the solutions.

This paper focuses on rotationally symmetric configurations, where C_{2n} is fixed to zero. Nonetheless, N_{2n} introduced in (31) has strong analogies to C_{2n}.

The coefficient N_{2n} is a nonlinear property of the system (because it is measured on the limit-cycle with amplitude A^{st}): it is the $2n\theta$ component of the nonlinear, amplitude dependent gain $\text{Re}[Q]$ that affects the stability of standing modes:

1. If $N_{2n} < 0$, standing solutions are not stable
2. If $N_{2n} > 0$, standing solutions are stable

In experiments, one can measure N_{2n} as

$$N_{2n} = \int_0^{2\pi} \text{Re}[Q_\theta^{\text{st}}] \sin(2n\theta) d\theta \qquad (33)$$

---

[5] we use here a slightly different notation and definition of C_{2n} for simpler comparison with the conventions adopted in this paper, though the same exact role/meaning of [9] holds.

[6] i.e. transfer function

where the frame of reference is chosen such that $p(t)$ has a pressure anti-node at $\theta = \pi/4$, and Q_θ^{st} is the transfer function between local values of heat release rate and pressure fluctuations, calculated from the data of a self-excited annular combustor experiencing a stable[2] standing mode with azimuthal wavenumber[4] n.

## EXAMPLE: THERMOACOUSTIC TRIGGERING IN ANNULAR COMBUSTORS

In this section we consider an example of application, for an annular combustor with a non-trivial flame response, as opposed to the simpler heat release models used so far in the literature. We have noticed that it is the real part of the describing function that plays the dominant role in determining the amplitudes of the solutions, see equations (24,27). This in turn depends on nonlinear gain and phase response. It is possible to show that both the gain and the phase dependence on amplitude can explain the occurrence of stable standing solutions.

In this example we focus on the effect of the gain. To isolate this effect, we fix the dependence of the phase response ϕ to be constant, $\phi(A, \omega) = \pi/5$. To make the example more compelling, we use as flame response the data from [26], which is an experimental and modelling study of a thermoacoustic system exhibiting a subcritical instability, i.e. triggering. The instantaneous spatially integrated OH-chemiluminescence response of the experiment is reported with black dots for a run of the experiment in Figure 4.a, as a function of the longitudinal velocity at the burner. Notice how the response is initially linear, then drops a little approximately between 0.5 and 0.8, to then regain strength at larger amplitudes at around 1. This figure does not contain any information about the phase response, which we are keeping constant. We assume that the heat release response is proportional to the OH-chemiluminescence, and extract the gain of the response as

$$G(\hat{u}/u) = \frac{|\hat{I}_{\text{OH}}|/\bar{I}_{\text{OH}}}{|\hat{u}|/\bar{u}} \qquad (34)$$

We are going to study the problem in non-dimensional time, so that the period of the thermoacoustic oscillation is 2π, and $\omega = 1$. Under the hypothesis of acoustically compact burners, we have that $G(A) \propto G(\hat{u}/u)$, where A is the amplitude of oscillation of the pressure at the burner's location in the chamber. We scale the gain G, reported in Figure 4.b with a black line, both horizontally and vertically:

1. the horizontal scaling occurs because at the burner $\hat{p} = Z(\omega)\hat{u}$; since we do not have the exact impedance value we rescale it so that the pressure amplitude of oscillation is in the range $[0, 1]$;
2. the vertical scaling is carried out to account for typical growth-rates/damping coefficient values of annular combus-
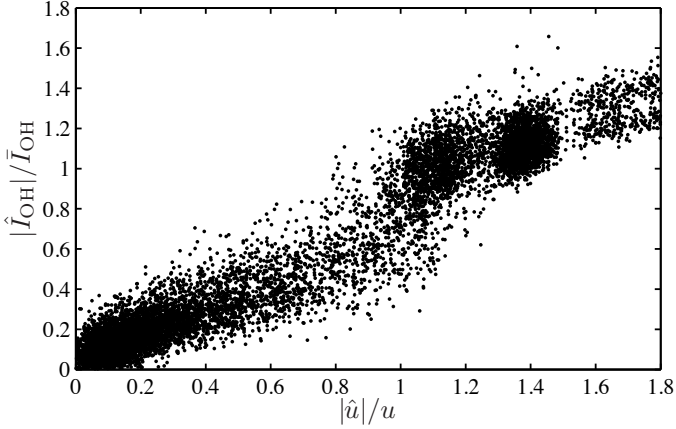
(a) INSTANTANEOUS FLAME RESPONSE IN THE SELF-EXCITED EXPERIMENT [26]
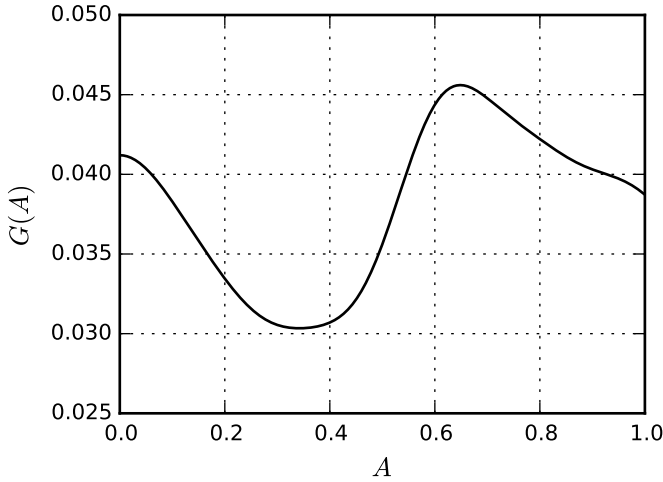
(b) EXTRACTED GAIN OF THE FLAME RESPONSE

FIGURE 4: a) INSTANTANEOUS AMPLITUDES OF THE DOMINANT FOURIER COMPONENT OF OH-CHEMILUMINESCENCE AND OF THE LONGITUDINAL VELOCITY AT THE BURNER'S POSITION, TAKEN FROM [26]. b) EXTRACTED GAIN USING EQUATION (34). THE RESULT HAS THEN BEEN SCALED IN BOTH AXES A AND G.

tors in nondimensional frequency units, obtained from experimental data, see e.g. [27].

Notice how in Figure 4.b the gain G first drops, to then increase again before decreasing with the amplitude A.

We now fix the number of burners N_b to 6, and study 2 combustors that differ only in the amount of acoustic damping α_1, α_2. The amplitudes of the spinning and standing solutions are the solutions of the equations (24,27). We study these equations as function of the maximum amplitude R_{max}, in time and space, as

introduced in equation (23). We present in Figure 5 the LHS of the equations (24,27): *1)* the function $F^{sp}(R_{max})$ in blue to discuss spinning modes; *2)* the function $F^{st,0}(R_{max})$ in red, to discuss the standing mode with a pressure anti-node at the location of one burner ($\zeta = 0$); *3)* the function $F^{st,2}(R_{max})$ in magenta, to discuss the standing mode with a pressure anti-node located exactly between 2 consecutive burners ($\zeta = 2$).

The solutions are the intersections of these curves with the horizontal black lines at the 2 ordinates α_1, α_2, reported with dashed and dashed-dotted lines in Figure 5. We can use the conditions (29,30) to discuss the stability of the solutions, and we plot each of them with a filled/empty circle if the solution is respectively stable/unstable.

We first define 2 critical values of damping, reported in the Figure with 2 horizontal black lines:

$$\alpha_l \equiv F^{sp}(0) = F^{st,\zeta}(0) \qquad (35)$$
$$\alpha_h \equiv \max\{F^{sp}\} \qquad (36)$$

Notice how we do not have data about the flame response at amplitudes larger than 1. We assume that the response decreases monotonically with amplitude there when we calculate α_h in (36). We can define 3 ranges of study for the damping coefficient α:

1. if $\alpha < \alpha_l$, one can prove with a linear stability analysis on (12) that the fixed point is linearly unstable;
2. if $\alpha_l < \alpha < \alpha_h$ the fixed point is linearly stable, but there exist standing and spinning solutions at large amplitudes of oscillation. The system is capable of thermoacoustic triggering;
3. if $\alpha_h < \alpha$ the fixed point is linearly stable, and we cannot find standing or spinning solutions. The system is globally stable, in the sense that the damping is large enough to kill off completely thermoacoustic instabilities.

The first value of damping $\alpha_1 = 0.085$ in Figure 5 belongs to the first case, while the second value of damping $\alpha_2 = 0.105$ belongs to the second case. Notice how at $\alpha = \alpha_1$ the only stable solution is of spinning type, while at $\alpha = \alpha_2$ both standing and spinning solutions are stable.

We can carry out the same analysis for any value of the damping α, reported in Figure 6.a. We omit the horizontal lines corresponding to the different values of the damping, and we draw the functions F with a thick/thin line wherever these solutions are respectively stable/unstable. As expected, the acoustic damping coefficient α strongly affects the amplitude of the solutions, but it also affects the type of stable solutions.

We stress that the 3 functions F are not plotted for amplitudes larger than 1, because there is no data available at these amplitudes. If the response of the flame Q decreases monotoni-
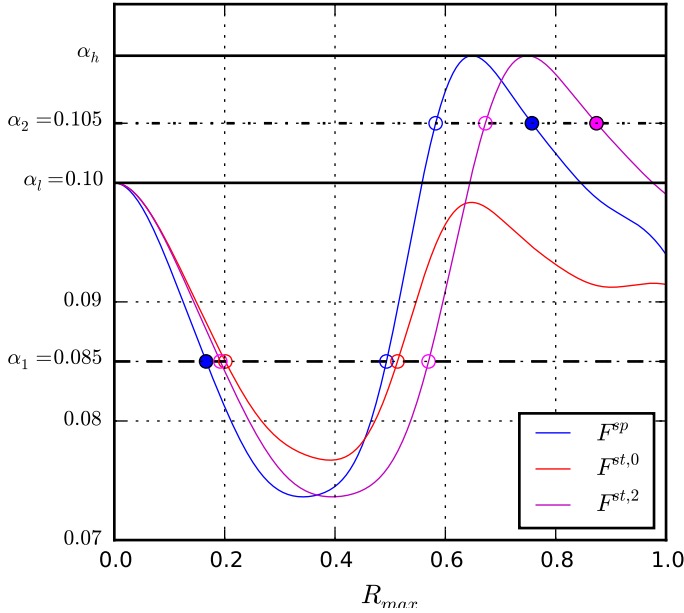
FIGURE 5: AMPLITUDE OF OSCILLATION R_{max} OF SPINNING (BLUE) AND STANDING (RED/MAGENTA) SOLUTIONS FOR A COMBUSTOR EQUIPPED WITH 6 BURNERS. WE CONSIDER 2 COMBUSTORS THAT DIFFER ONLY IN THE ACOUSTIC DAMPING COEFFICIENT α, REPORTED WITH THE 2 HORIZONTAL BLACK LINES. THE SOLUTIONS ARE CIRCLES, WHICH ARE FILLED/EMPTY IF THE SOLUTION IS STABLE/UNSTABLE.

cally with amplitude, we have for example that at $\alpha = \alpha_1$ there will be 3 more solutions at amplitude larger than 1.

We can then generalize the analysis to any number of burners N_b. We present in Figure 6 the result for $6, 7, 8, 9$ burners, for an arbitrary value of the damping. We observe that the stability and the amplitudes of the standing modes is strongly affected by the number of burners.

This example shows how a flame that responds with a weak gain at low amplitudes (in the linear regime) and with a stronger gain at larger amplitudes (closer to the saturated amplitude of a standing solution), because it respects the condition (33), can present stable standing solutions. These occur only if the system can exhibit triggering, hence the strong dependence on the damping coefficient α. Moreover, the condition (33) is only a simpler and approximate abstraction to look at the stability of standing solutions, because the number of burners N_b affects the exact position of the burners along the annulus in the stability conditions (30b,30c).

Notice how this is just one example of stable standing solutions, and we are not here implying that thermoacoustic triggering is a necessary condition for stable standing solutions to occur.

CONCLUSIONS

We discuss azimuthal thermoacoustic oscillations in annular combustors. The key assumptions of this work are: *1)* there is no effect of transverse forcing and no adjacent flames' interaction; *2)* only one degenerate pair of modes of azimuthal nature oscillates; *3)* the weakly nonlinear formalism is applicable; *4)* the flames are acoustically compact.

The amplitude of spinning solutions is fixed by the Rayleigh criterion at the limit-cycle. The same criterion provides also the condition for stable spinning solutions: the energy balance must be negative at larger amplitudes of oscillation, as for thermoacoustic oscillations in longitudinal configurations.

Also the amplitude of standing solutions is fixed by the Rayleigh criterion at the limit-cycle. However, the same criterion provides only 1 of 3 stability conditions for standing solutions: the energy balance must be negative at larger amplitudes of oscillation.

There are 2 more conditions for stable standing solutions:

1. the condition (30b) discusses the stability of a standing mode with respect to a rotation of its velocity nodal line in the azimuthal direction. This condition disappears for the case with a large number of burners N_b, in which every azimuthal orientation is allowed for standing solutions;
2. we show that the azimuthal Fourier component 2θ of the part of the flame response in phase with the pressure in a limit-cycle of a standing solution, called N_{2n} and defined in (31), is the most stringent condition for a large number of burners N_b. If N_{2n} is positive there exist stable standing solutions. This conjecture can be tested from experimental data of stable standing solutions to validate the hypotheses of this theory.

We then present an example of the analysis that shows that an annular combustor capable of thermoacoustic triggering can present stable standing solutions. We predict amplitudes and stability of the spinning and standing solutions, parametrically in the damping coefficient α and in the number of burners N_b of the combustor.

We obtained some implications for industrial annular combustors as well. The occurrence of stable standing solutions is related either: *1)* with a non-rotationally symmetric combustor; *2)* with a flame response that is weak at small amplitudes and strong at large amplitudes, so that the condition (31) holds; *3)* with other physical mechanisms, such as for example transverse forcing, dynamical temperature effects, or the effect of a mean azimuthal flow on the flame response.

REFERENCES

[1] Staffelbach, G., Gicquel, L., Boudier, G., and Poinsot, T., 2009. "Large Eddy Simulation of self excited azimuthal modes in annular combustors". *Proceedings of the Combustion Institute,* ***32***(2), pp. 2909–2916.

[2] Poinsot, T., Wolf, P., Staffelbach, G., Gicquel, L. Y. M., and Muller, J. D., 2011. "Identification of azimuthal modes in annular combustion chambers". *Annual research briefs. Center for Turbulence Research.*, pp. 249–258.

[3] Wolf, P., Staffelbach, G., Gicquel, L. Y., Müller, J.-D., and Poinsot, T., 2012. "Acoustic and Large Eddy Simulation studies of azimuthal modes in annular combustion chambers". *Combustion and Flame,* ***159***(11), Nov., pp. 3398–3413.

[4] Moeck, J. P., Paul, M., and Paschereit, C. O., 2010. "Thermoacoustic instabilities in an annular Rijke tube". *Proceedings of ASME turbo expo 2010, paper no. GT2010-23577.*

[5] Worth, N. A., and Dawson, J. R., 2013. "Modal dynamics of self-excited azimuthal instabilities in an annular combustion chamber". *Combustion and Flame,* ***160***, June, pp. 2476–2489.

[6] Worth, N. A., and Dawson, J. R., 2013. "Self-excited circumferential instabilities in a model annular gas turbine combustor: Global flame dynamics". *Proceedings of the Combustion Institute,* ***34***, Jan., pp. 3127–3134.

[7] Bourgouin, J.-F., Durox, D., Moeck, J. P., Schuller, T., and Candel, S., 2013. "Self-sustained instabilities in an annular combustor coupled by azimuthal and longitudinal acoustic modes". *Proceedings of ASME Turbo Expo 2013, paper no. GT2013-95010.*

[8] Bourgouin, J.-F., Durox, D., Moeck, J. P., Schuller, T., and Candel, S., 2015. "Characterization and Modeling of a Spinning Thermoacoustic Instability in an Annular Combustor Equipped With Multiple Matrix Injectors". *Journal of Engineering for Gas Turbines and Power,* ***137***, Sept., p. 021503.

[9] Noiray, N., Bothien, M. R., and Schuermans, B., 2011. "Investigation of azimuthal staging concepts in annular gas turbines". *Combustion Theory and Modelling,* ***15***(5), Oct., pp. 585–606.

[10] Ghirardo, G., and Juniper, M., 2013. "Azimuthal instabilities in annular combustors : standing and spinning modes". *Proceedings of the Royal Society A: Mathematical, Physical and Engineering Sciences,* ***469***.

[11] Schuermans, B., Paschereit, C. O., and Monkewitz, P., 2006. "Non-Linear Combustion Instabilities in Annular Gas-Turbine Combustors". In 44th AIAA Aerospace Sciences Meeting and Exhibit. Paper no. AIAA-2006-0549, American Institute of Aeronautics and Astronautics.

[12] Stow, S. R., and Dowling, A. P., 2009. "A Time-Domain Network Model for Nonlinear Thermoacoustic Oscillations". *Journal of Engineering for Gas Turbines and Power,*
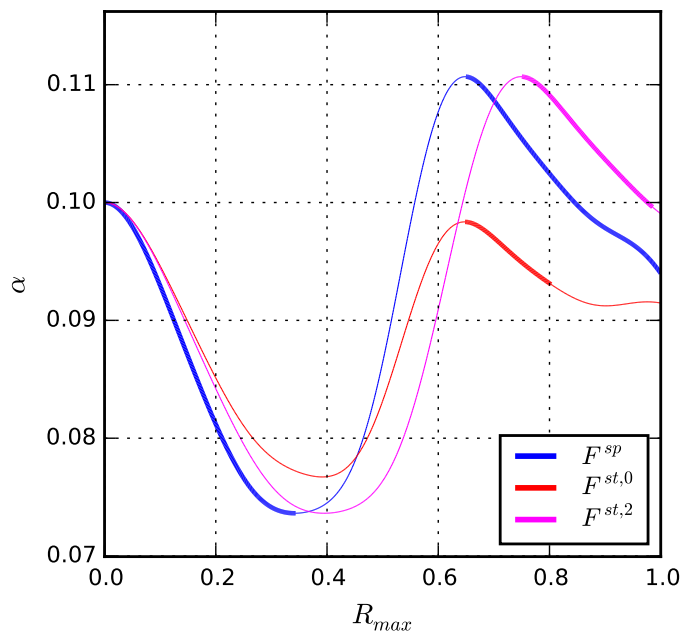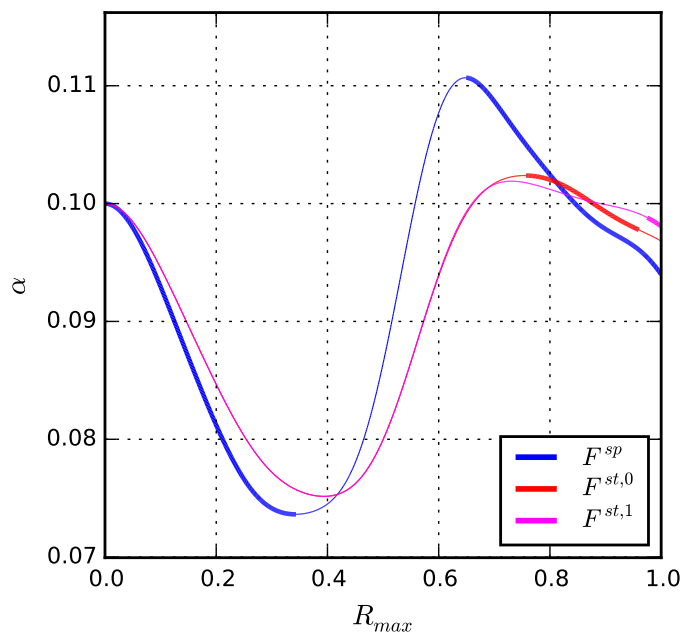
(a) $N_b = 6$
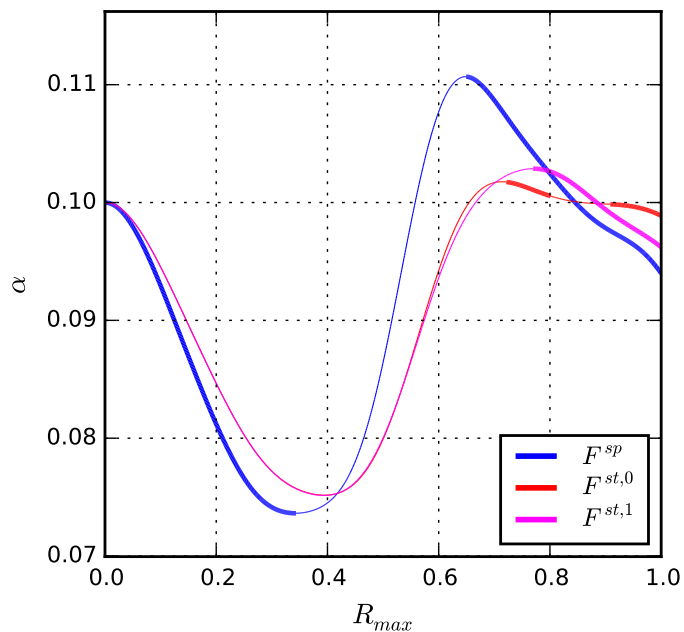
(b) $N_b = 7$
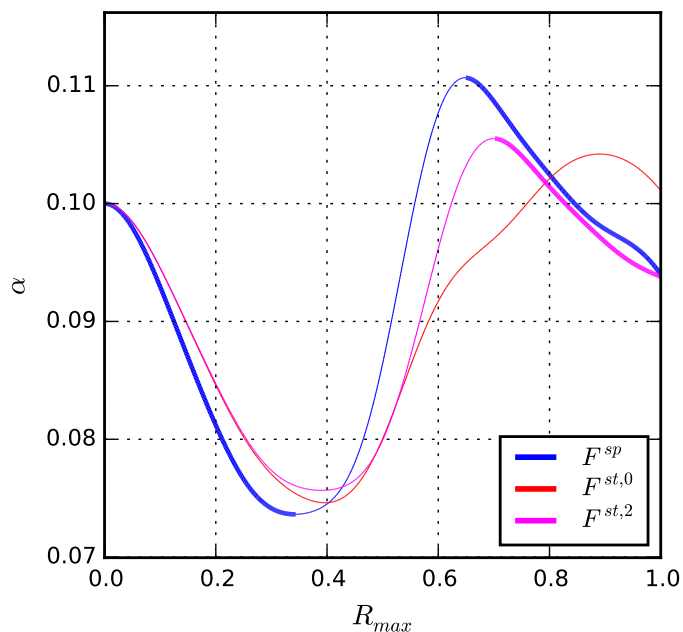
(c) $N_b = 8$

(d) $N_b = 9$

FIGURE 6: STABILITY MAP AS A FUNCTION OF THE DAMPING COEFFICIENT α. THE NUMBER OF BURNERS N_b IS DIFFERENT IN EACH OF THE SUB-FIGURES. THIS ANALYSIS IS A GENERALIZATION OF FIGURE 5 FOR ALL VALUES OF THE DAMPING COEFFICIENT α. THE LINES ARE THICK/THIN IF THE RESPECTIVE SOLUTION IS STABLE/UNSTABLE.

$\mathbf{131}$(3), p. 031502.

[13] Noiray, N., and Schuermans, B., 2013. "On the dynamic nature of azimuthal thermoacoustic modes in annular gas turbine combustion chambers". *Proceedings of the Royal*

Society A: Mathematical, Physical and Engineering Sciences, 469, Jan.

[14] Bauerheim, M., Cazalens, M., and Poinsot, T., 2015. "A theoretical study of mean azimuthal flow and asymmetry effects on thermo-acoustic modes in annular combustors". *Proceedings of the Combustion Institute, 35*, June, pp. 3219–3227.

[15] Acharya, V., Shreekrishna, Shin, D.-H., and Lieuwen, T., 2012. "Swirl effects on harmonically excited, premixed flame kinematics". *Combustion and Flame, 159*(3), Mar., pp. 1139–1150.

[16] Acharya, V., and Lieuwen, T., 2014. "Response of non-axisymmetric premixed, swirl flames to helical disturbances". In Proceedings of ASME Turbo Expo 2014. Paper no. GT2014-27059.

[17] Saurabh, A., Steinert, R., Moeck, J. P., and Paschereit, C. O., 2014. "Swirl flame response to traveling acoustic waves". In Proceedings of ASME Turbo Expo 2014. Paper no. GT2014-26829.

[18] OConnor, J., and Acharya, V., 2013. "Development of a flame transfer function framework for transversely forced flames". *Proceedings of ASME Turbo Expo 2013, paper no. GT2013-95900*.

[19] Blimbaum, J., Zanchetta, M., Akin, T., Acharya, V., OConnor, J., Noble, D., and Lieuwen, T., 2012. "Transverse to longitudinal acoustic coupling processes in annular combustion chambers". *International Journal of Spray and Combustion Dynamics, 4*(4), pp. 275–298.

[20] Ćosić, B., Moeck, J. P., and Paschereit, C. O., 2014. "Nonlinear Instability Analysis for Partially Premixed Swirl Flames". *Combustion Science and Technology, 186*(6), May, pp. 713–736.

[21] Gelb, A., and Vander Velde, W., 1968. *Multiple input describing functions and nonlinear system design*. McGraw-Hill Book.

[22] Schuller, T., Durox, D., and Candel, S., 2003. "A unified model for the prediction of laminar flame transfer functions". *Combustion and Flame, 134*(1-2), July, pp. 21–34.

[23] Nicoud, F., Benoit, L., Sensiau, C., and Poinsot, T., 2007. "Acoustic Modes in Combustors with Complex Impedances and Multidimensional Active Flames". *AIAA Journal, 45*(2), Feb., pp. 426–441.

[24] Durox, D., Bourgouin, J.-F., Moeck, J. P., Philip, M., Schuller, T., and Candel, S., 2013. "Nonlinear interactions in combustion instabilities coupled by azimuthal acoustic modes". In (International summer school and workshop on non-normal and nonlinear effects in aero- and thermoacoustics), June 18-21, 2013, Munich.

[25] Bourgouin, J.-F., 2014. "Dynamique de flamme dans les foyers annulaires comportant des injecteurs multiples". PhD thesis, Ecole Centrale Paris.

[26] Moeck, J. P., Bothien, M. R., Schimek, S., Lacarelle, A., and Paschereit, C. O., 2008. "Subcritical thermoacoustic instabilities in a premixed combustor". In 14th AIAA/CEAS Aeroacoustics Conference, paper no. AIAA-2008-2946, no. May.

[27] Bothien, M. R., Noiray, N., and Schuermans, B., 2014. "Analysis of azimuthal thermoacoustic modes in annular gas turbine combustion chambers". In Proceedings of ASME Turbo Expo 2014. Paper no. GT2014-25903.